Quiescent times in Gamma-Ray-Bursts: hints of a dormant inner engine

Alessandro Drago[1,2] & Giuseppe Pagliara[3,2]

ABSTRACT

We perform a statistical analysis of the temporal structure of long Gamma-Ray-Bursts (GRBs). First we consider a sample of bursts in which a long quiescent time is present. Comparing the pre-quiescence with the post-quiescence emission we show that they display similar temporal structures, hardness ratios and emitted powers, but, on the average, the post-quiescence emission is roughly twice as long as the pre-quiescence emission. We then consider a sample of long and bright GRBs. We show that the duration of each emission period is compatible with the duration of an active period computed in various inner engine models. At the contrary, if the inner engine is assumed to be always active, i.e. also during the quiescent times, in several cases the total duration of the burst largely exceeds the theoretical durations. Our analysis therefore does not support the interpretation of long quiescent times in terms of stochastic modulation of a continuous wind. Instead the quiescent times can be interpreted as dormancy periods of the inner engine. Before and after a dormancy period the inner engine produces similar emissions.

Subject headings: gamma rays: bursts – dense matter

1. Introduction

The time structure of GRBs is usually complex and it often displays several short pulses separated by time intervals lasting from fractions of second to several ten of seconds. The analysis of the light curves can provide hints on the activity of the inner engine although the relation between the observed signal and the Physics of the inner engine is not yet completely understood.

[1]Dipartimento di Fisica, Università di Ferrara, 44100 Ferrara, Italy

[2]INFN, Sezione di Ferrara, 44100 Ferrara, Italy

[3]Dipartimento di Fisica, Politecnico di Torino, 10129 Torino, Italy

A previous statistical analysis (Nakar & Piran 2002b) has shown that there are three time-scales in the GRB light curves: the shortest one is the variability scale determining the pulses' durations and the intervals between pulses; the largest one describes the total duration of the bursts and, finally, an intermediate time scale is associated with long periods within the bursts having no activity, the so called *quiescent times* [1]. The origin of these periods of quiescence is still unclear.

Here we show, through a statistical analysis, that if a quiescent time longer than a few ten of seconds is present in the light curve then the pre-quiescence and the post-quiescence emissions (PreQE, PostQE) have similar variability scales but, on the average, the PostQE is longer and only marginally softer than the PreQE. The similarities between the first and the second emission periods strongly suggest that both emissions are produced by the same mechanism. Moreover we will show that the average durations of PreQE and of PostQE, separately, are compatible with the theoretical durations predicted by various inner enngine models.

2. Data analysis

We have performed a statistical analysis of the time intervals Δt between adjacent peaks using the peak finding algorithm of Li & Fenimore (1996) and borrowing from Nakar & Piran (2002a) the definition of active periods separated by Quiescent Times (QTs). In Fig. 1 we show an example of burst where the previous quantities are illustrated. We have applied this analysis to all the light curves of the BATSE catalogue.

In a first investigation we have merged all the bursts of the catalogue into one sample from which we compute the cumulative probability $c(\Delta t)$ of finding time intervals Δt which are not QTs i.e. we compute the distribution of the time intervals within each active period. In Fig. 2a, we show that $c(\Delta t)$ is well described by a log-normal distribution. In Fig. 2b, the histogram of QTs is displayed together with a log-normal distribution. As already observed by previous authors (Nakar & Piran 2002b), there is an evident deviation of the data points respect to the log-normal distribution for time intervals longer than a few seconds, indicating an excess of long Δt. In Fig. 2c we show a power law fit of the tail of the QTs distribution which displays a very good agreement with the data, as already observed by Quilligan et al. (2002). The physical interpretation of this distribution will be discussed later. Finally, in

[1] QTs are not the same as the gaps between the precursors and the main pulses. In the case of the precursors, the gaps are between a softer and weaker component (the precursor) and a harder and much stronger one (the main burst). Here we observe gaps between pulses with the same characteristics.

Fig. 2d we show a correlation function, indicating the probability of finding at least 2 QTs longer than ΔT in a same GRB. As shown in the figure this probability rapidly decreases and it essentially vanishes for $\Delta T > 40$ s.

A technical remark. In our analysis we have considered two possible values for σ, the parameter used to discriminate signal from noise. A standard choice is $\sigma = \sqrt{background}$. Using that definition we can reproduce the results of Nakar & Piran (2002b) on the cumulative distribution of Δt. Instead, the results presented in our figures have been obtained using another definition: $\sigma = \sqrt{\mathrm{Max}}$, where Max is the maximum number of counts in the light curve. The reason for this choice is that we want to study the main events of a GRB light curve (the ones having a large luminosity) and not the faint micro-structures (as for instance precursors, which we would exclude from our sample). It is important to remark that, using this larger value of σ we can recover the main results of Nakar and Piran, but the distinction between a) time intervals which are not QTs and b) QTs is now even more clear on a statistical basis: the firsts are perfectly interpreted by a lognormal distribution, while long QTs are very well fitted by a power-law, as discussed before.

We can now define a subsample of the BATSE catalogue composed of all the bursts having a QT longer than 40 s [2]. In Fig. 2a we also show the distribution of Δt within the subsample. The distributions of the full BATSE catalogue and of the subsample are essentially equal. This indicates that the subsample is not composed of bursts having an anomalously large redshift because instead all time scales within the subsample would be homogeneously dilated.

In our analysis we will now concentrate on the subsample. From the result of Fig. 2d, the bursts of the subsample contain only one long QT and it is therefore possible to divide each burst into a PreQE and a PostQE of which we will compare the temporal and spectral structure.

In Fig. 3 we display the cumulative distributions $c_1(\Delta t)$ and $c_2(\Delta t)$ within each of the two emission periods. In panel a we display only Δt which are not QTs (same as in Fig. 2a), while in panel b QTs are included. In both cases the two distributions are very similar. The χ^2-test provides a significance of 28% for panel a and of 34% for panel b that the two data sets are drawn from the same distribution function [3]. Let us remind that within

[2]The subsample contains the following 36 GRBs of BATSE catalogue: 142, 222, 869, 1328, 1989, 2138, 2148, 2156, 2211, 2213, 2922, 3336, 3351, 3488, 3634, 3776, 5421, 5478, 5486, 5585, 6295, 6335, 6454, 6472, 6629, 6745, 6892, 7170, 7185, 7301, 7503, 7549, 7769, 8001, 8063, 8087.

[3]The χ^2-test has been performed on the set of Δt after a binning and not on the cumulative distribution. We have checked that using binnings in the range 2–8 s the result of the test remains stable.

the internal-external-shocks model (Piran 2004; Zhang & Meszaros 2004), external shocks produce emissions lacking the short time scale variability produced by internal shocks (Sari & Piran 1997). The result of Fig. 3 rules out a scenario in which PostQE is dominated by external shocks and PreQE by internal shocks. This in turn excludes the possibility of associating the QTs with the time needed to the jet to reach and interact with the interstellar medium. Clearly enough, the statistical analysis we are presenting does not rule out the existence of specific GRBs in which the second episode is indeed associated with external shocks. For instance GRB960530 and GRB980125 are examples of bursts in which PostQE has a smoother morphology and a softer spectral evolution than PreQE (Hakkila & Giblin 2004).

We perform now a statistical analysis of the durations $D1$ and $D2$ of the two emission periods. As shown in Fig. 4a, the two data sets are well fitted by two log-normal distributions (the Kolmogorov-Smirnov test provides a significance of $\sim 90\%$). The two distributions have different mean values ($D1_{ave} \sim 21s$, $D2_{ave} \sim 41s$) and almost identical standard deviations ($\sigma_1 = 36s$, $\sigma_2 = 33s$). We address now the following question: is the longer duration of PostQE a manifestation of a progressive increase in the active periods' durations during the burst? To answer this question we have repeated the previous analysis by dividing PreQE and PostQE each in two parts, using the longest QT within each emission as a divider. The distributions of the duration of all parts are shown in Fig. 4b. The durations of the two parts within each emission period share the same distribution (the χ^2-test provides significances larger than 50% in both cases) but, in agreement with the previous findings, the average durations of the two parts of PostQE are longer than the two parts of PreQE. Therefore, the longer duration of PostQE cannot be attributed to a continuous modification of the emission but is a specific feature of the second part of the GRB.

To estimate the emitted energy during PreQE and PostQE we have analyzed the hardness ratios, defined as the ratios between the photon counts in two BATSE channels (the second and the third in our case). The average hardness of PostQE turns out to be only marginally smaller ($\sim 20\%$) than the average hardness of PreQE. Since, as shown above, the average durations of PreQE and of PostQE are in the relation $D2_{ave} \sim 2\, D1_{ave}$, the total energy emitted during PostQE is also about a factor of 2 larger than the one emitted during PreQE. This is also evident from the result of Fig. 5, where the distributions of the powers emitted during PreQE and PostQE are displayed, showing that the average powers of the two emissions are essentially the same.

It is interesting to compare our result on the durations with the correlation between duration of QT and of PostQE found by Ramirez-Ruiz et al. (2001a). By computing the average duration of QT and of PostQE in our subsample (which is not the same analyzed

by those authors) we obtain the following result: PostQE $\sim$ 41 s and QT $\sim$ 80 s. Therefore, in our sample and using the Nakar and Piran algorithm we cannot confirm the correlation found by Ramirez-Ruiz et al. (2001a). Indeed, if that correlation was present the average durations of QT and of PostQE should be comparable, since the correlation law suggested by those authors is a straight line with a slope of order one. Actually, in our sample the statistical correlation between the durations of QT and of PostQE is very small, $r \sim 0.13$.

3. Discussion

3.1. Dormant engine scenario *vs.* wind modulation model

As observed by Ramirez-Ruiz et al. (2001b), within the internal shocks model it is possible to explain the QTs either as a turn-off of the IE or as a modulation of a continuous relativistic wind emitted by the IE (Wind Modulation Model WMM). Both hypothesis are consistent with the result of Fig. 3.

The main difference between the WMM and the dormant engine scenario is that in the WMM the inner engine has to provide a constant power during the whole duration of the burst. In our subsample, we have several bursts whose total duration (including the QT) approaches 300 s. These durations have to be corrected taking into account the average redshift of the BATSE catalogue, $z_{ave} \sim 2$ (Piran 1999), but even after this renormalization, durations of a hundred seconds or more are not too rare. This time scale has to be compared with the typical duration of the emission period of the inner engine, as estimated in various models. For instance, in all numerical investigations of the collapsar model (MacFadyen & Woosley 1999; Zhang et al. 2003) the IE remains switched-on during some 20s. There is at the moment no indication that a "steady state disk", characterized by a mass infall rate large enough to power the GRB, can last hundreds of seconds instead of tens of seconds. Also in the quark deconfinement model (Cheng & Dai 1996; Bombaci & Datta 2000; Ouyed & Sannino 2002; Berezhiani et al. 2003; Paczynski & Haensel 2005) the inner engine remains active during periods of the order of a few ten seconds corresponding to the cooling time of the compact stellar object.

To better clarify our argument concerning both the duration of an emission period and the energy injected by the inner engine, let us first discuss an example of a bright and long burst, GRB #7301 of the BATSE catalogue (see Fig. 7). In that burst a large QT is present lasting $\sim$ 100 s followed by a PostQE of $\sim$ 70 s and with a PreQE of $\sim$ 40 s. To compare these time-scales to the typical durations provided by the models for the inner engine we have first to divide all the observed durations by a factor of 3, due to the average redshift of

the BATSE catalogue. While the resulting durations of PreQE and of PostQE are then in agreement with the typical time duration of an emission period in the collapsar model or in the quark deconfinement model ($\sim$ 20 s), the total duration of the burst ($\sim$ 73 s, including the QT lasting $\sim$ 35 s), is roughly a factor of three larger than the duration in the theoretical models. It is therefore difficult to explain the long duration of the total burst within the current inner engine models if the WMM is adopted.

Obviously, the previous remark would be meaningless if the example we are providing is not typical of the time structure of long GRBs. Instead, by checking all the GRBs of the "current catalogue" of BATSE, having $T_{90} > 100$ s and peak photon flux in the 256 ms channel > 5 photons^{-1}cm^{-2}, we can come to the following conclusion: all the lightcurves of this subsample can be interpreted within the dormant engine model by rescaling the total duration by a factor 1/(z+1) = 1/3 and by splitting the burst in two emission episodes, separated by a dormancy period corresponding to a chosen QT. In Figs. 6,7 we show all the GRBs of this sample and we indicate the longest QT. Clearly enough, there are bursts in which it is not unambiguous to decide which QT has to be interpreted as the dormancy period, because more than one long QT is present. In the Figure we indicate the only two cases (out of 15 GRBs analyzed) in which we suggest a dormancy period which is different from the longest QT. In both those cases the suggested dormancy period corresponds to the second longest QT present in the burst. This rather small ambiguity can easily be explained by noticing that a small fraction of long QTs can be generated by stochastic fluctuations (described by the tail of the log-normal distribution) and not by a dormancy period. As discussed above, the association of a QT with a dormancy period is totally unambiguous for bursts in which a QT longer than $\sim$ 40 s is present. The last light curve presented in Fig. 7 (GRB # 6454) corresponds to a faint burst which does not belong to the subsample discussed in this section (GRBs of high luminosity). It is interesting to notice that in this burst PreQE and PostQE are so long that also after dividing their durations by a redshift factor of three, the durations are not compatible with the existing IE models. Anyway, the faintness of this burst is probably due to the extreme distance of the source and a larger red-shift correction should then be applied. Similar considerations are also valid for other superlong bursts presented in Tikhomirova & Stern (2005) (GRB # 6454 is one of the burst discussed in that paper). [4]

[4]Using the algorithm of Nakar & Piran (2002a) some faint components of the lightcurves are not considered as parts of the signal because their counts number is smaller than 4-5 σ and therefore they cannot be considered as active periods. This reflects on the estimated duration of the bursts. In particular there are bursts whose T_{90} durations exceed 100 s, while their durations based on the active periods are shorter and therefore these bursts are excluded from our sample. This selection criteria clearly depends on the value of σ. We have performed our analysis using for σ both choices described in Sec. 2. In Figs. 6-7 we show the results

Another problem with the WMM is due to the prevision, within that model, that the emitted power during PostQE is larger than during PreQE. This prevision is based again on the existence of a continuous emission of shells also during the QT (Ramirez-Ruiz et al. 2001b). The analysis displayed in Fig. 5 does not support this prevision.

It is also worth recalling that, on the average, PostQE lasts roughly twice PreQE. While it is probably possible to fix the parameters of the WMM so to satisfy that constraint, no reason is provided within the WMM model to explain that feature in terms of the activity of the inner engine or of the dynamics of the jet formation. At the contrary, models for a dormant inner engine can associate the durations of the emission periods with the durations of physical phenomena taking place within the IE. This point will be discussed in the next Section.

We conclude that long QTs most probably correspond to periods of inactivity of the IE. On the other hand, it is possible that the WMM is responsible for short QTs occurring within the two emission periods, as suggested by Fig. 4b where it is shown that the durations of the two parts of a single emission period have the same distribution. Finally, while our subsample is composed of GRBs having QTs longer than 40 s, it is surely possible that in many cases the IE switches-off for a much shorter time. Unfortunately, in those cases it is not trivial to distinguish between QTs generated by the switch-off and QTs generated by the WMM, as it also results from the discussion of Figs. 6,7.

3.2. Models for a dormant inner engine

Let us now discuss how to generate dormancy periods using various models of the IE. Within the most popular model, the collapsar model (MacFadyen & Woosley 1999), there are two possible scenarios: a temporary interruption of the jet produced by Kelvin-Helmhotz instabilities (Woosley et al. 2003) or the fragmentation of the collapsing stellar core before its merging with the black hole (King et al. 2005). In both scenarios it can be possible to produce long QTs. For instance, in the scenario proposed by King et al. (2005) the durations of the emission periods are related to the durations of the accretion disks generated by each fragment. Our result on the durations of PreQE and of PostQE can be explained if, e.g., the average mass of the second fragment is larger than that of the first fragment. A discussion

---

obtained using $\sigma = \sqrt{background}$, which is the most conservative choice (in this case the excluded GRBs are # 1157, # 1886, # 3458, # 3930, # 7527). Using instead the larger value for σ, further components of the lightcurves would be excluded, and our conclusions would be even stronger.

of the mass distribution of the fragments can be found in Perna et al. (2006) [5].

Another model for the IE is based on the conversion of a metastable hadronic star into a star containing quark matter (Cheng & Dai 1996; Bombaci & Datta 2000; Ouyed & Sannino 2002; Berezhiani et al. 2003; Paczynski & Haensel 2005). In the last years the possibility of forming a diquark condensate at the center of a compact star has been widely discussed in the literature (Rajagopal & Wilczek 2000). The formation of a color superconducting quark core can increase the energy released by a significant amount (Drago et al. 2004). It has also been shown that the conversion from normal to gapped quark matter goes through a first order transition (Ruster et al. 2005). It is therefore tempting to associate PreQE with the transition from hadronic to normal quark matter and PostQE with the formation of the superconducting phase (Drago et al. 2005). In this scenario the two dimensional scales regulating the durations of PreQE and PostQE are the energies released in the two transitions. Finally, let us remark that the power-law fitting the long QTs distribution can originate from a superposition of exponential distributions with different decay times (Wheatland 2000). In the quark deconfinement model, the different decay times are associated with slightly different masses of the metastable compact star. If the interpretation based on the quark deconfinement model is correct then the GRBs data analysis provides very stringent bounds on the physics of high density matter.

A possible signature of the models in which the IE goes dormant would be the detection of external shock emissions at the end of both PreQE and PostQE, indicating that the two emissions are physically disconnected.

4. Conclusions

In this paper we have studied the problem of quiescent times in long GRBs borrowing the technique developed by Nakar and Piran. The main results obtained in our analysis are the following:

— the cumulative distribution of time intervals between peaks within a same active period is well fitted by a lognormal distribution, while long quiescent times are well fitted by a pow-

[5]Disk fragmentation models could explain the recent X-ray-flare observations by Swift (Burrows et al. 2005) which suggests the possibility of a re-brightening of the IE. In those cases, however, the detected signal was softer than the GRB prompt emission (the X-ray flares have not been detected by the BAT instrument on Swift, but by the XRT). The re-brightening phenomena which we call PostQEs belong instead to the prompt emission and they are only marginally softer then the PreQEs. X-ray flares belong therefore to another class of phenomena.

erlaw distribution. This strengthens Nakar & Piran (2002b) conclusion about the different origin of long quiescent times respect to shorter time intervals;

— the two components of the emission, preceding and following the quiescent time are statistically similar from the viewpoint of their temporal microstructure, their hardness ratio and emitted power. These results suggest a unique mechanism at the origin of both the pre-quiescence and the post-quiescence emission. Interestingly, the second emission lasts on the average twice the first, what provides an important constraint to the inner engine models;

— the durations of the activity periods of the inner engine, computed within the existing theoretical models do not exceed few ten seconds. These theoretical estimates compare favorably with the durations of the pre-quiescent and of the post-quiescent emissions, separately. On the other hand, in several bursts the total duration including the quiescent time, is roughly three times longer. This is an indication in favor of a dormant inner engine respect to wind modulation models.

5. Acknowledgments

It is a pleasure to thank Filippo Frontera, Enrico Montanari and Rosalba Perna for many useful suggestions and for help in the data analysis.

REFERENCES

Berezhiani, Z., Bombaci, I., Drago, A., Frontera, F. & Lavagno, A., 2003, Astrophys.J., 586, 1250

Bombaci I. & Datta B., 2000, Astrophys.J., 530, L69

Burrows, D.N. et al. 2005, Science 309, 1833

Cheng, K.S.& Dai Z.G., 1996, Phys.Rev.Lett., 77, 1210

Drago, A., Lavagno, A. & Pagliara, G., 2004, Phys.Rev., D69, 057505

Drago, A., Lavagno, A. & Pagliara, G., 2005, astro-ph/0510018, Proceedings QM2005, August 2005 Budapest.

Hakkila, J. & Giblin, T.W., 2004, Astrophys.J., 610, 361

King, A., O'Brien, P.T., Goad, M.R., Osborne, J., Olsson, E. & Page, K., 2005, Astrophys.J., 630, L113

Li, H. & Fenimore, E., 1996, Astrophys.J., 469, L115

MacFadyen, A.L. & Woosley, S.E., 1999, Astrophys.J., 524, 262

Nakar, E. & Piran, T., 2002a, Mon. Not. Roy. Astron. Soc., 330, 920

Nakar, E. & Piran, T., 2002b, Mon. Not. Roy. Astron. Soc., 331, 40

Ouyed, R. & Sannino, F., 2002, Astron. Astrophys., 387, 725

Paczynski, B. & Haensel, P., 2005, Mon. Not. Roy. Astron. Soc. Lett., 362, L4

Perna, R., Armitage, P.J. & Zhang, B., 2006, Astrophys.J., 636, L29

Piran, T., 1999, Phys.Rept., 314, 575

Piran, T., 2004, Rev.Mod.Phys., 76, 1143

Quilligan, F., McBreen, B., Hanlon L., McBreen S., Hurley K.J. & Watson D., 2002, Astron. & Astrophys., 385, 377

Rajagopal, K. & Wilczek, F., 2000, hep-ph/0011333.

Ramirez-Ruiz, E., Merloni, A., 2001, Mon. Not. Roy. Astron. Soc., 320, L25

Ramirez-Ruiz, E., Merloni, A. & Rees, M.J., 2001, Mon. Not. Roy. Astron. Soc., 324, 1147

Ruster, S.B. , Werth, V., Buballa, M., Shovkovy, I.A. & Rischke, D.H., 2005, Phys. Rev. D73, 034025

Sari, R. & Piran, T 1997, Astrophys.J., 485, 270

Tikhomirova , Y. & Stern, B 2005, Astron. Lett. 31, 291

Wheatland, M.S., 2000, Astrophys. J., 536, L109

Woosley, S.E., Zhang, W. & Heger A., 2003, AIP Conference Proceedings, 662, 185

Zhang, B. & Meszaros, P., 2004, Int.J.Mod.Phys., A19, 2385

Zhang, W., Woosley, S.E. & MacFadyen, A.I.., 2003, Astrophys. J., 586, 356

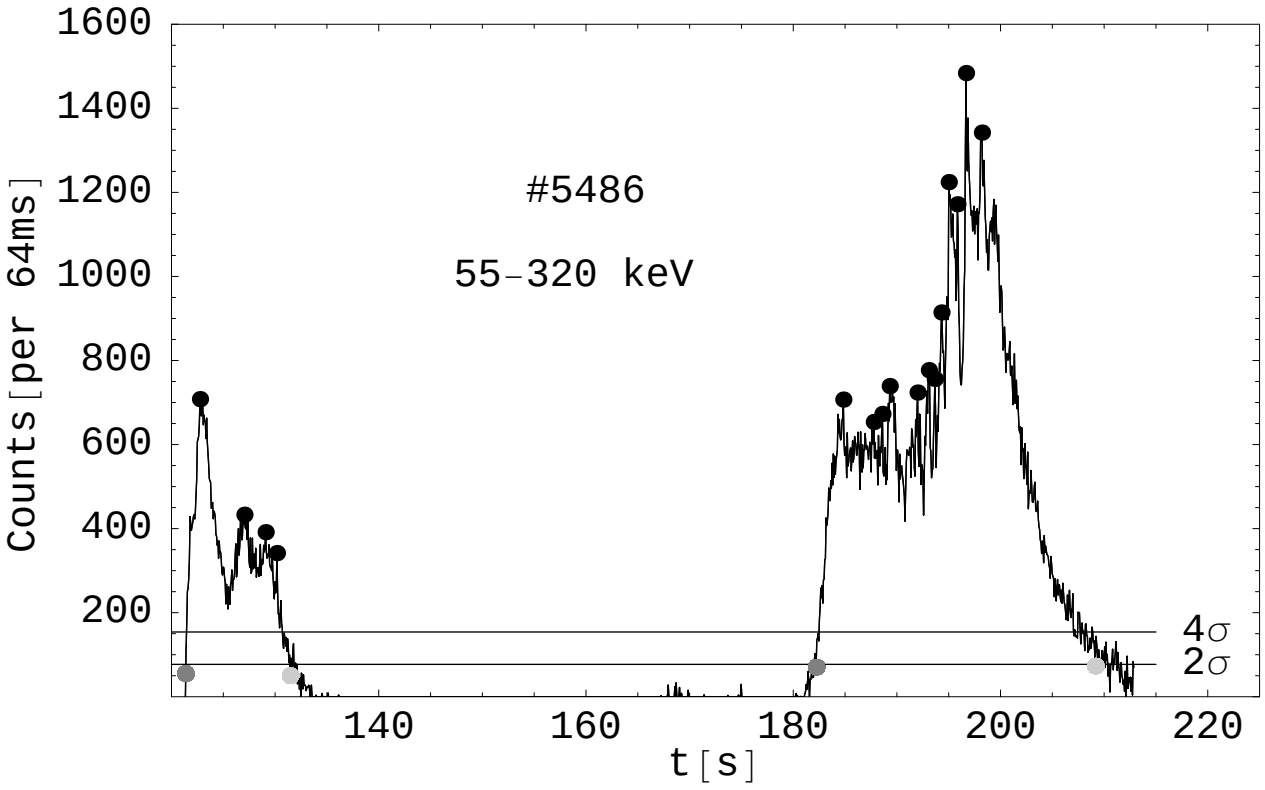

Fig. 1.— **Light curve of a typical GRB** Time profile of BATSE burst #5486 in the energy range $55Kev < E < 320Kev$. For each light curve, the background is first determined using a linear fit and then subtracted from the data. The signal is extracted taking as initial and final bins the ones with counts above 2σ. The active periods are defined as periods in which bins with counts exceeding 4σ are present. Active periods begin (dark-gray dots) and end (light-gray dots) when the signal drops below 2σ. Within each active period we search for peaks using the peak finding algorithm of Li & Fenimore (1996): indicating with C_p the counts of a candidate peak and with C_1 and C_2 the counts in the bins to the left and to the right of the candidate, a "true" peak must satisfy the relations $C_p - C_{1,2} \geq N_{var}\sqrt{C_p}$, where $N_{var} = 5$ in our analysis. The true peaks are indicated by the black points.

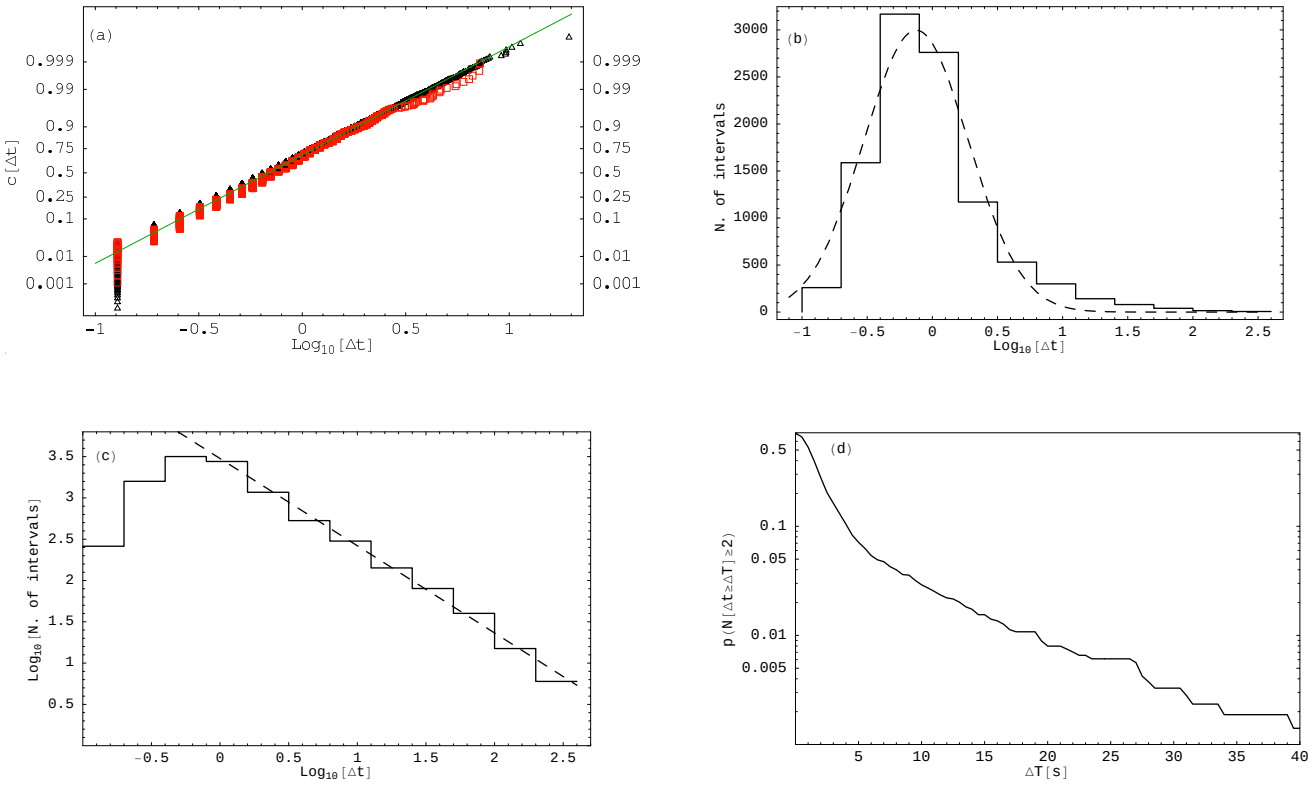

Fig. 2.— **Analysis of time intervals between peaks a** The cumulative distribution of time intervals Δt which are not QTs (black triangles), is compared with its best fit log-normal distribution (solid green line). The data come from the full BATSE sample after eliminating bursts displaying data gaps. The boxes correspond to the cumulative distribution of Δt taken from the subsample of bursts containing a QT longer than 40s (see text). **b** Histogram of the QTs and its log-normal fit (dashed line). **c** Histogram of QTs and power-low fit of its tail (dashed line). The fit is based only on QTs longer than 40s. **d** Frequency of bursts containing at least two QTs longer than ΔT.

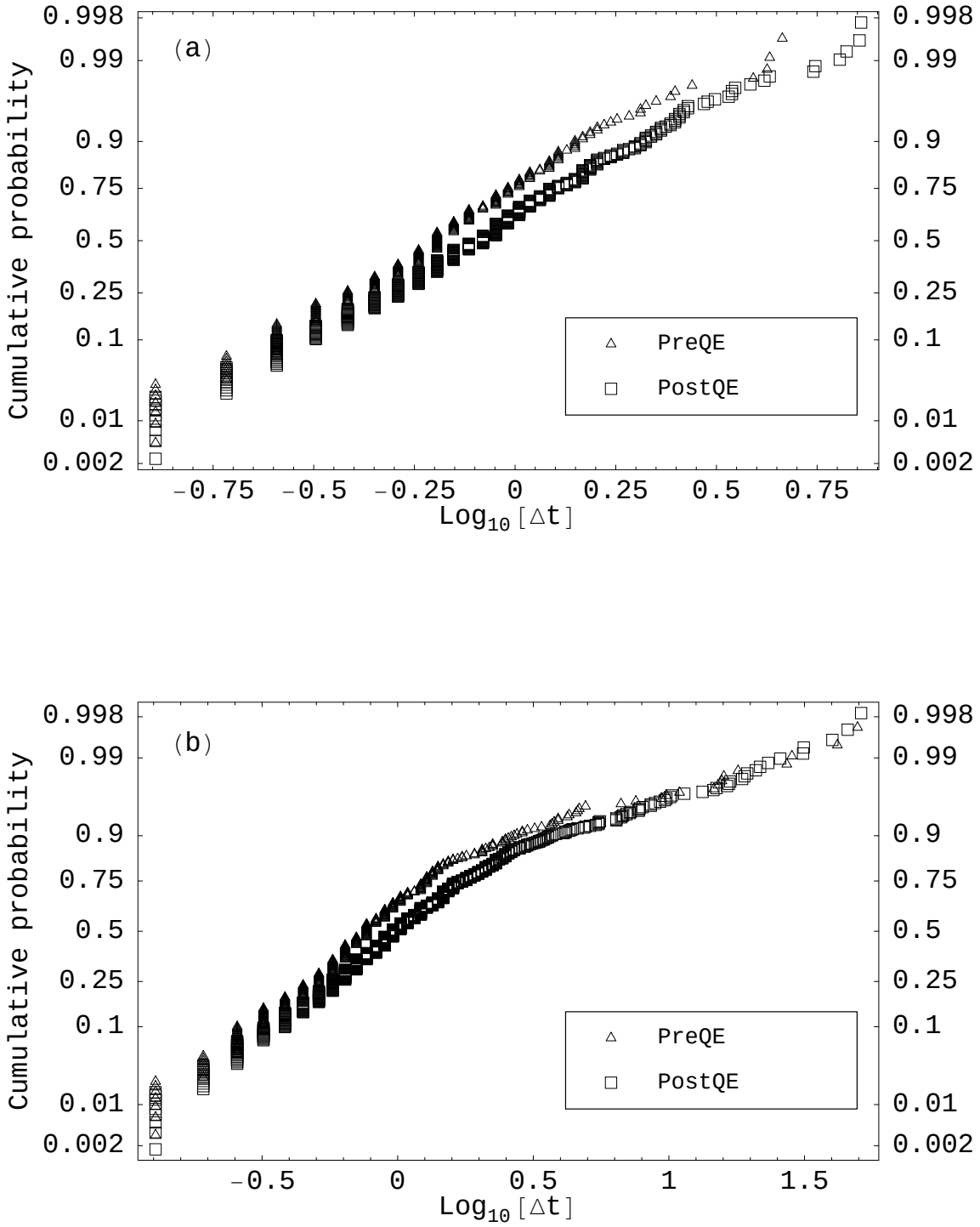

Fig. 3.— **Analysis of time intervals between peaks within the two emission periods a** The cumulative distribution of time intervals Δt which are not QTs are shown for the two emission episodes, PreQE and PostQE. **b** The cumulative distributions of Δt are shown for the two emission episodes including QTs.

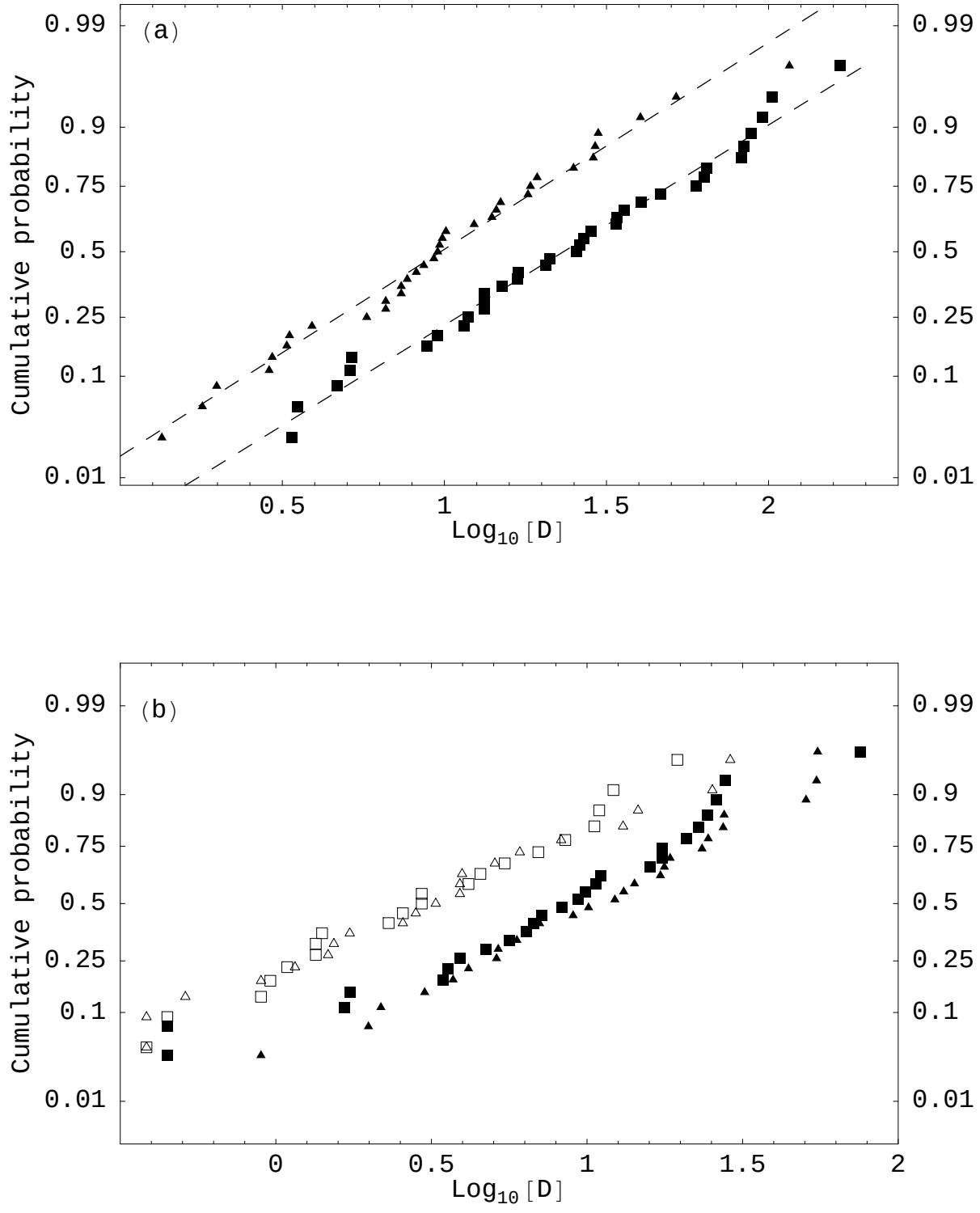

Fig. 4.— **Analysis of the durations D of the two emission periods a** Cumulative distributions of durations of PreQE (filled triangles) and of PostQE (filled boxes) and their best-fit log-normal distributions (dotted lines). **b** Cumulative distributions of durations of the first and second part of PreQE (empty triangles and boxes) and of PostQE (filled triangles and boxes).

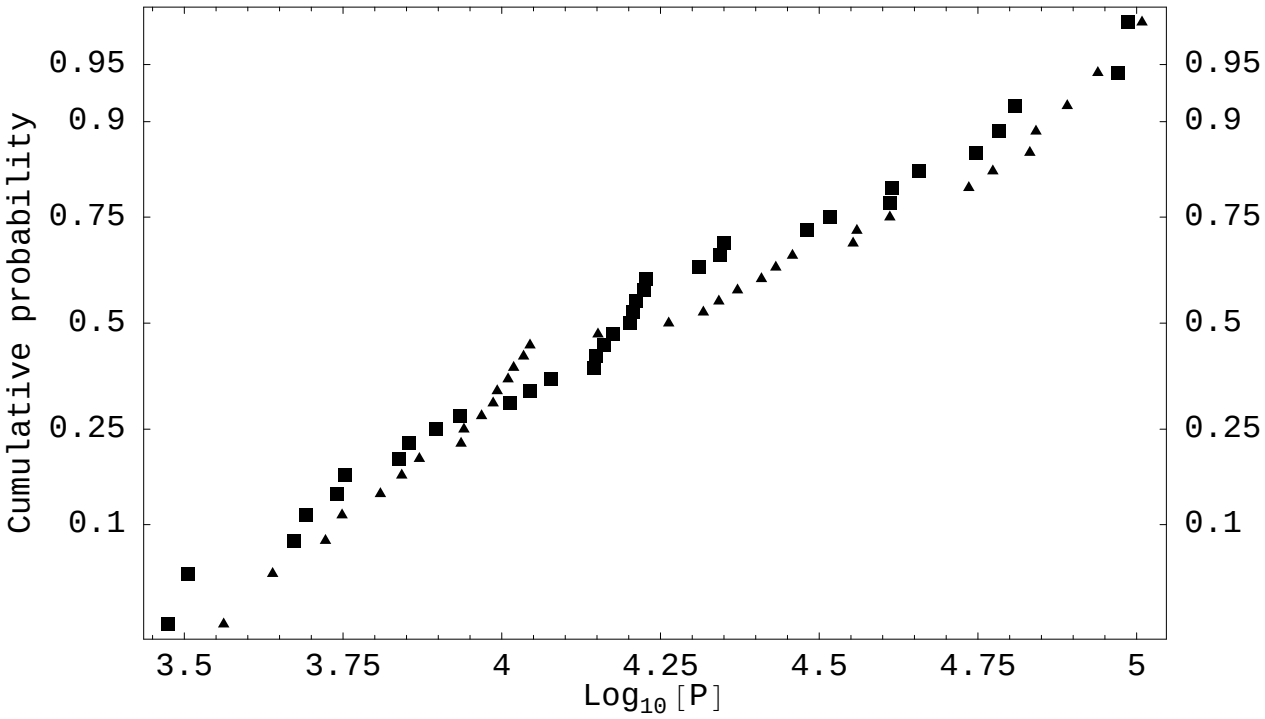

Fig. 5.— **Analysis of the powers P of the two emission periods** Cumulative distributions of powers of PreQE (filled triangles) and of PostQE (filled boxes)

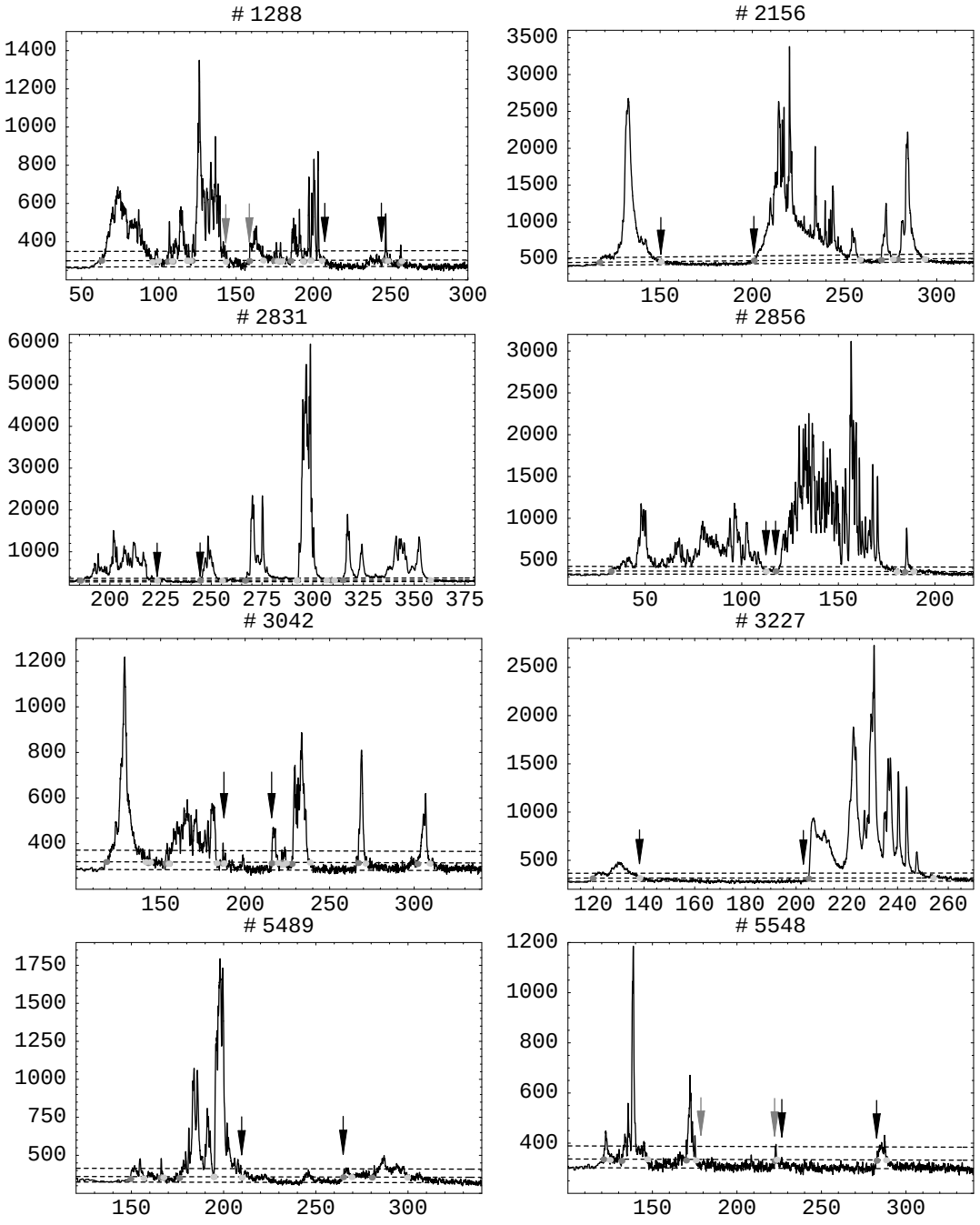

Fig. 6.— **Long and bright bursts** GRBs of the "current catalogue" of BATSE, having $T_{90} > 100$ s and peak photon flux in the 256 ms channel > 5 photons^{-1}cm^{-2}. The dashed lines indicate the fit of the background and the 2σ and 5σ levels used to define the active periods. Dark-gray dots and light-gray dots mark the initial and the end point of each active period, respectively. Black arrows indicate the longest QT. Gray arrows indicate the suggested dormancy period when it does not coincide with the longest QT (two cases only).

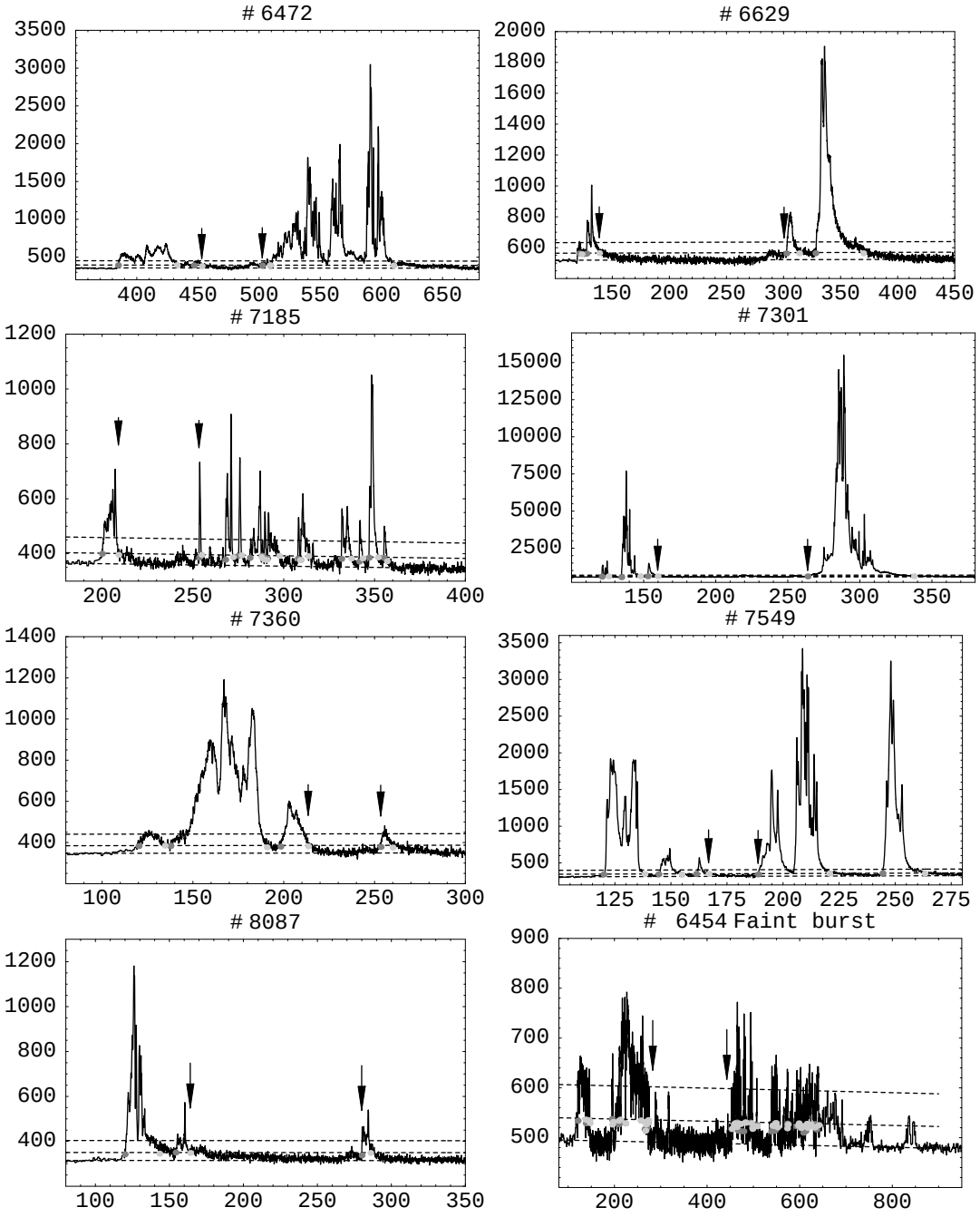

Fig. 7.— **Long and bright bursts** Same as in Fig. 6. Here the suggested dormancy period always coincide with the longest QT. We also display a faint burst # 6454 (it does not satisfy the limit on the peak photon flux) whose very long duration could be due to a large red-shift.